ARTICLE
Journal of Cellular Biochemistry 113:3342–3352 (2012)

Journal of Cellular Biochemistry

Hypoxia Modulation of Peroxisome Proliferator-Activated Receptors (PPARs) in Human Glioblastoma Stem Cells. Implications for Therapy

Renato Galzio,[1] Loredana Cristiano,[2] Alessia Fidoamore,[2] Maria Grazia Cifone,[1] Elisabetta Benedetti,[2] Benedetta Cinque,[1] Paola Menghini,[1] Sohelia Raysi Dehcordi,[1] Rodolfo Ippoliti,[2] Antonio Giordano,[3,4**] and Annamaria Cimini[1,4*]

[1]*Department of Health Sciences, University of L'Aquila, L'Aquila, Italy*
[2]*Department of Basic and Applied Biology, University of L'Aquila, L'Aquila, Italy*
[3]*Department of Pathology and Oncology, University of Siena, Siena, Italy*
[4]*Sbarro Institute for Cancer Research and Molecular Medicine, Temple University, Philadelphia, Pennsylvania*

ABSTRACT

Gliobastoma (GB), the most common adult brain tumor, infiltrates normal brain area rendering impossible the complete surgical resection, resulting in a poor median survival (14–15 months), despite the aggressive multimodality treatments post-surgery, such as radiation and chemo-therapy. GB is characterized by hypoxic and necrotic regions due to a poorly organized tumor vascularization, leading to inadequate blood supply and consequently to hypoxic and necrotic areas. We have previously shown that, under hypoxia GB primary cells increased the expression of stemness markers as well as the expression of the nuclear receptor peroxisome proliferator-activated receptor α (PPARα) and also the crucial role played by PPARs in mouse neural stem cells maintenance and differentiation. Due to the importance of lipid signaling in cell proliferation and differentiation, in this work, we analyzed the expression of PPARs in GB neurospheres both in normoxic and hypoxic conditions. The results obtained suggest a differential regulation of the three PPARs by hypoxia, thus indicating a possible therapeutic strategy to counteract GB recurrencies. J. Cell. Biochem. 113: 3342–3352, 2012.

KEY WORDS: HYPOXIA; PPARs; GLIOBLASTOMA STEM CELLS

The crucial role played by the cellular microenvironment in the modulation of tumor behavior is raising great attention. Reduced oxygen level in the affected areas is a feature of many tumors, especially tumors with high proliferation rate [Bar et al., 2010]. Gliobastoma (GB), the most common adult brain tumor, infiltrates normal brain area rendering impossible the complete surgical resection, resulting in a poor median survival (14–15 months), despite the aggressive multimodality treatments post-surgery, such as radiation, and chemo-therapy [Benedetti et al., 2010b; Cimini and Ippoliti, 2011]. GB is characterized by hypoxic and necrotic regions due to a poorly organized tumor vascularization, leading to inadequate blood supply and consequently to hypoxic and necrotic areas [Amberger-Murphy, 2009; Bar, 2011]. Hypoxia has been related to the poor outcome of the patients [Vaupel and Mayer, 2007; Sathornsumetee et al., 2008; Jensen, 2009], since it hypoxic/necrotic tumors are more resistant to chemotherapy and radiation therapies [Amberger-Murphy, 2009]. This may be related to the fact that hypoxia is known to support non-neoplastic neural stem cells, raising the possibility that "cancer stem cells" may also be affected by oxygen levels [Panchision, 2009]. In fact, in cultured cells, oxygen levels play an important role in regulating cellular differentiation [Panchision, 2009]. Growth under low oxygen concentrations is known to maintain pluripotency, and to inhibit the differentiation of embryonic stem cell [Ezashi et al., 2005]. In agreement, it has been shown that hypoxia increases stemness markers in GB-derived neurospheres, such as CD133, SOX2, nestin, and Oct4 [Sahlgren et al., 2008; Sathornsumetee et al., 2008; McCord et al., 2009; Pistollato et al., 2009; Soeda

*Correspondence to: Annamaria Cimini, Department of Basic and Applied Biology, University of L'Aquila, via Veotio n. 10, 67100 L'Aquila, Italy. E-mail: annamaria.cimini@univaq.it
**Correspondence to: Antonio Giordano, Sbarro Institute for Cancer Research and Molecular Medicine, Temple University, Philadelphia, PA. E-mail: president@shro.org
Manuscript Received: 22 May 2012; Manuscript Accepted: 23 May 2012
Accepted manuscript online in Wiley Online Library (wileyonlinelibrary.com): 29 May 2012
DOI 10.1002/jcb.24210 • © 2012 Wiley Periodicals, Inc.

et al., 2009]. We have previously shown that, under hypoxia GB primary cells increased the expression of stemness markers as well as the expression of a nuclear receptor, namely peroxisome proliferator-activated receptor α (PPARα) [Benedetti et al., 2008, 2010b]. Moreover, we have previously reported the possible crucial role played by PPARs in mouse neural stem cells maintenance and differentiation [Cimini et al., 2007; Cimini and Cerù, 2008]. It has been also reported that PPARγ ligands regulate neural stem cells proliferation and differentiation both in vitro and in vivo [Morales-Garcia et al., 2011], while recently it has been suggested that PPARγ-mediated advanced glycation end products is involved in neural stem cells proliferation [Wang et al., 2011]. PPARs are ligand-activated transcription factors belonging to the nuclear hormone receptor superfamily (Nuclear Receptor Nomenclature Committee, 1999). Three related isotypes have been described so far, the PPARα (NR1C1), the PPARβ/δ (NR1C2) [Issemann and Green, 1990], and the PPARγ (NR1C3) [Dreyer et al., 1992]. PPARs exhibit a wide but isotype-specific tissue expression pattern which can account for the variety of cellular functions they regulate [Escher and Wahli, 2000].

PPARs may be considered sensors capable of adapting gene expression to lipid signals. The diversity of functions in which they are involved is also reflected by the diversity of ligands that can be bind in their ligand binding pocket. In fact, PPARs are activated by a wide range of naturally occurring lipids or their metabolites derived from the diet or from intracellular signaling pathways, which include saturated and unsaturated fatty acids and fatty acid derivatives, such as prostaglandins and leukotriens [Krey et al., 1997; Berger and Moller, 2002]. PPARs activate the transcription of their target genes as heterodimers with retinoid X receptors (RXR, NR2B) [Keller et al., 1993; Wolfrum et al., 2001]. All three RXR isotypes (α, β, and γ) can dimerize with PPARs, and specific association with each isotype seems to influence the recognition of target gene promoters [Gearing et al., 1993]. All three PPAR isotypes are involved in the regulation of cell proliferation, death, and differentiation, with different roles and mechanisms depending on the specific isotype and ligand and on the undifferentiated, differentiated, or transformed status of the cell. Thus, proliferative and antiapoptotic or antiproliferative, prodifferentiating and proapoptotic effects, and even anticarcinogenic or procarcinogenic effects have been reported for PPARs [Feige et al., 2006]. PPARs are involved in different important pathways present also in the control of the proliferation, migration, and differentiation of NSC, that is, Wnt signaling pathway, STAT3 and NFkB pathways [Doherty, 2007; Guillemot, 2007; Garza et al., 2008].

We have recently reported in GB primary cultures that hypoxia increases both stemness markers and PPARα expression [Laurenti et al., 2011], raising the possibility that hypoxia may directly or indirectly modulate PPARα activation and consequently lipid metabolism. Due to the importance of lipid signaling in cell proliferation and differentiation, in this work, we analyzed the expression of PPARs in GB neurospheres both in normoxic and hypoxic conditions. The results obtained suggest a differential regulation of the three PPARs by hypoxia, thus indicating a possible therapeutic strategy to counteract GB recurrencies.

MATERIALS AND METHODS

Triton X-100, dimethylsulfoxide (DMSO), sodium dodeciylsulfate (SDS), Tween 20, bovine serum albumin (BSA), HOECHST, Nonidet P40, sodium deoxycolate, ethylene diamine tetraacetate (EDTA), phenylmethanesulphonylfluoride (PMSF), sodium fluoride, sodium pyrophosphate, ortovanadate, leupeptin, aprotinin, pepstatin, NaCl, polyvinylidene difluoride (PVDF) sheets, anti-PMP70, anti-SDNSF, glycerol, acetone, fluorescein-labeled anti-rabbit and anti-mouse IgG antibodies, Triacylglycerol (1,2 dimyrystoil-3 palmytoil-rac-glycerol) (TAG), trimyrystin (TRIM), tripalmytoil (TRIP), cholesterol (C) were all purchased from Sigma Chemical CO (St. Louis, CO). Micro-BCA kit was purchased Pierce Biotechnology (Rockford, IL). Anti-AOX was purchased Chemicon (Nuernberg, Germany), anti PPARα was from Affinity Bioreagents, Inc. (Golden, CO), Horseradish peroxidase (HRP)-conjugated anti-mouse or anti-rabbit IgG secondary antibodies were from Santa Cruz Biotechnology (Santa Cruz, CA). Enhanced chemiluminescence (ECL) Bio-Rad Laboratories, (Hercules, CA). Trizol reagent was purchased from Invitrogen (Paisley, UK). High-Capacity cDNA Reverse Trascription Kit, TaqMan universal PCR master mix and Assay on Demand gene expression reagents for human ACOX1, HMGCoA-Red, THIO, PPARα, PPARβ, PPARγ TATA Box-Binding Protein (TBP) were all purchased from Applied Biosystems (Foster City, CA). All other chemicals were of the highest analytical grade.

CELL CULTURE

U87 Glioblastoma cells (ATCC) were cultured, according to Yu et al. [2008], with minor modification. Briefly, U87 cells were cultured in Dulbecco's Modified Eagle's Medium (DMEM; Sigma–Aldrich, St. Louis, MO) supplemented with 10% fetal bovine serum (FBS), 2 mM glutamine, 0.1 mg/ml penicillin, and 0.1 mg/ml streptomycin (Sigma) and incubated at 37°C in humidified 95% air−5% CO_2 atmosphere. Thereafter, U87 the culture medium was replaced with serum-free neural stem cell medium, Dulbecco's Modified Eagle's Medium-F12 (DMEM-F12; Sigma), containing 20 ng/ml of both recombinant human epidermal growth factor (EGF) and fibroblast growth factor-basic (b-FGF; PeproTech, Hamburg, Germany) until several tumorsphere were visible under microscopy. After several passages primary tumorspheres were dissociated and single cells were seeded at 1×10^4/well. The secondary spheres derived from single cells of primary tumorspheres were analyzed under phase contrast microscopy Leica DMIL and fluorescence microscopy Zeiss Axioplan 2, with Leica DFC 350 FX camera.

HYPOXIA INDUCTION PROCEDURE

Hypoxic stress was exerted by placing culture dishes in an airtight chamber. The chamber was sealed and the air was reduced to 0.5 Atm by aspiration and replaced by flushing for 30 min with a gas mixture of 95% N and 5% CO_2. The resultant atmosphere contained low oxygen concentration as monitored by the anerobic indicator BR55. To maintain the temperature at 37°C the chamber was returned to the incubator. The relative humidity was maintained as to close to 100% by filling the bottom of the chamber with deionized

sterile water. Hypoxic shock was applied for 72 h [Di Loreto et al., 2000].

PROTEIN ASSAY

Protein were assayed by the micro-BCA kit. Briefly, this assay is a detergent-compatible formulation based on bicinchoninic acid (BCA) for the colorimetric detection and quantitation of total protein. The method combines the reduction of Cu^2 to Cu^1 by protein in alkaline medium (the biuret reaction) with the high sensitive and selective colorimetric detection of the cuprous cation, using a reagent containing BCA [Smith et al., 1985]. The purple-colored reaction product of this assay is formed by the chelation of two molecules of BCA with one cuprous ion. This complex exhibits a strong absorbance at 562 nm.

PROLIFERATION ASSAY

Proliferation in control and treated cells was studied by following the incorporation of 5-bromo-2′-deoxy-uridine into cellular DNA (5-Bromo-2′-deoxy-uridine Labeling and Detection Kit III; Roche). The amount of BrdU incorporated is determined by a standard ELISA protocol, which involves ''tagging'' the incorporated nucleotide with an anti-BrdU antibody. Cells cultured in a 96-well microplate were incubated with BrdU. The labeled cells were then fixed with ethanol. Prior to incubation with a monoclonal antibody to BrdU, DNA was partially digested with nucleases to allow the antibody to access BrdU. Next, the anti-BrdU antibody, labeled with peroxidase (POD), was added. Finally, the POD substrate ABTS was added. POD catalyzes the cleavage of ABTS, producing a colored reaction product. The absorbance of the samples 405 nm is determined with a spectrophotometric microplate reader (Infinite F200 Tecan).

FLOW CYTOMETER ANALYSIS OF INTRACELLULAR PROTEINS AND CELL SURFACE ANTIGENS

Tumorsphere, grown in normoxic and hypoxic conditions for 72 h were dissociated and single-cell suspensions (0.5×10^6 cells/tube) were fixed for 15 min at RT with 2% formaldehyde in PBS. For intracellular protein staining (SOX2 GFAP, Nestin, HIF1α, SDNSF) cells were permeabilized for 5 min. at RT with 0.1% triton-X-100 in PBS. For extracellular staining (CD133) permeabilization was omitted. Non-specific binding sites were blocked incubating for 10 min at RT with 0,2% BSA in PBS. Cells were then incubated for 1 h at RT with primary antibodies diluted in PBS containing 0.2% BSA. The antibodies used in this study were: rabbit anti-CD133 (Abcam), anti-SOX2 (Abcam), anti-GFAP (Sigma) and mouse anti-Nestin, anti-SDNSF (Chemicon) anti-HIF1α (Novus Biologicals, Inc.). Cells were then washed with PBS containing 0.2% BSA and incubated for 1 h at RT with AlexaFluor 488 conjugated goat anti-rabbit or anti mouse IgG secondary antibodies (Molecular Probes, Invitrogen). After washing, cell suspensions were evaluated by flow cytometry using a FACSCalibur cytometer analyzer (Becton Dickinson, San Diego, CA) and data were analyzed using CellQuest software (BD).

WESTERN BLOTTING

Cells cultured in normoxia and hypoxia for 72 h were collected and lysated in ice-cold RIPA buffer (phosphate buffer saline pH 7.4 containing 0.5% sodium deoxycolate, 1% Nonidet P-40, 0.1% SDS, 5 mM EDTA, 100 mM sodium fluoride, 2 mM sodium pyrophosphate, 1 mM PMSF, 2 mM ortovanadate, 10 μg/ml leupeptin, 10 μg/ml aprotinin, 10 μg/ml pepstatin; Sigma). Protein lysates (20–30 μg) were separated on 7.5–15% SDS–polyacrilamide gel and electro-blotted onto polyvinyldifluoride membrane (PVDF; Sigma). Non-specific binding sites were blocked by 5% non-fat dry milk (Bio-Rad Laboratories, Hercules, CA) in Tris buffered saline (TBS: 20 mM Tris–HCl, pH 7,4, containing 150 mM NaCl) for 30 min at RT. Membranes were then incubated overnight at 4°C with following primary antibodies, all diluted with TBS containing 0,1% Tween 20 (TBS-T): rabbit anti-CD133 (1:500, Abcam), anti-SOX_2 (1:200), anti-HIF-1α (1:100; Santa Cruz, CA), anti-PMP70 (1:250) anti-GFAP (1:100), mouse anti-Nestin, anti-PPARα, β, and γ (1:200; Chemicon). As secondary antibodies peroxidase, conjugated anti-rabbit or anti mouse IgG (1:1,000; Vector Laboratories, Burlingame, CA). Immunoreactive bands were visualized by ECL (Pierce), according to the manufacturer's instructions. Immunoreactive bands relative densities were determined using TotalLab software (ABEL Science-Ware srl, Italy) and values were given as relative units (RU). Data were normalized to total protein load by quantification of all samples in a single assay before loading, and confirmation of equal loading by image analysis and scanned Coomassie blue-stained gels after blotting [Benedetti et al., 2010a].

REAL-TIME PCR

Total mRNA was harvested with the Trizol reagent according to the manufacturer's protocol. The gene expressions were quantified in a two-step reverse transcription-polymerase chain reaction (RT-PCR). Complimentary DNA was reverse transcribed from total RNA samples using High-Capacity cDNA reverse Trancription Kit. PCR products were synthesized from cDNA using the TaqMan universal PCR master mix and Assays on Demand gene expression reagents for human ACOX1, HMGCoA-Red, THIO, PPARα, PPARβ, PPARγ (Assay ID: Hs 00244515_m1, Hs00168352_m1, Hs00190073_m1, Hs00155616_m1, Hs00231882_m1, Hs00234592_m1, Hs00606407_m1). Measurements were made using the ABI Prism 7300HT sequence detection system, according to the manufacturer's protocol. As an endogenous control for these PCR quantification studies, TBP gene expression assay was used. Results represent normalized ACOX1, THIO, HMGCoA-Red, PPARα, PPARβ/δ, and PPARγ mRNA amounts relative to healthy tissue using the $2^{-\Delta\Delta C_t}$ method [Livak and Schmittgen, 2001]. Each experiment was repeated in triplicate.

IMMUNOFLUORESCENCE

Tumorspheres, grown in normoxic and hypoxic conditions for 72 h were seeded on poly-L-lysine coated coverslips (10 μg/ml; Sigma), fixed in 4% paraformaldehyde in PBS, for 10 min at RT and permeabilized with 0.1% Triton X-100 (Sigma) in PBS, for 5 min at RT. Non-specific binding sites were blocked with 3% BSA (Sigma) in PBS, for 10 min at RT. Tumorsphere were then incubated with following primary antibodies, overnight at 4°C: rabbit anti-Ki67 (Dako, Glostrup, Denmark), anti-CD133, and anti-SOX_2 (1:500; Abcam, Cambridge Science Park, Cambridge, UK), anti-PMP70 (1:250; Sigma), anti-PPARα, β, and γ (1:200; Affinity Bioreagent,

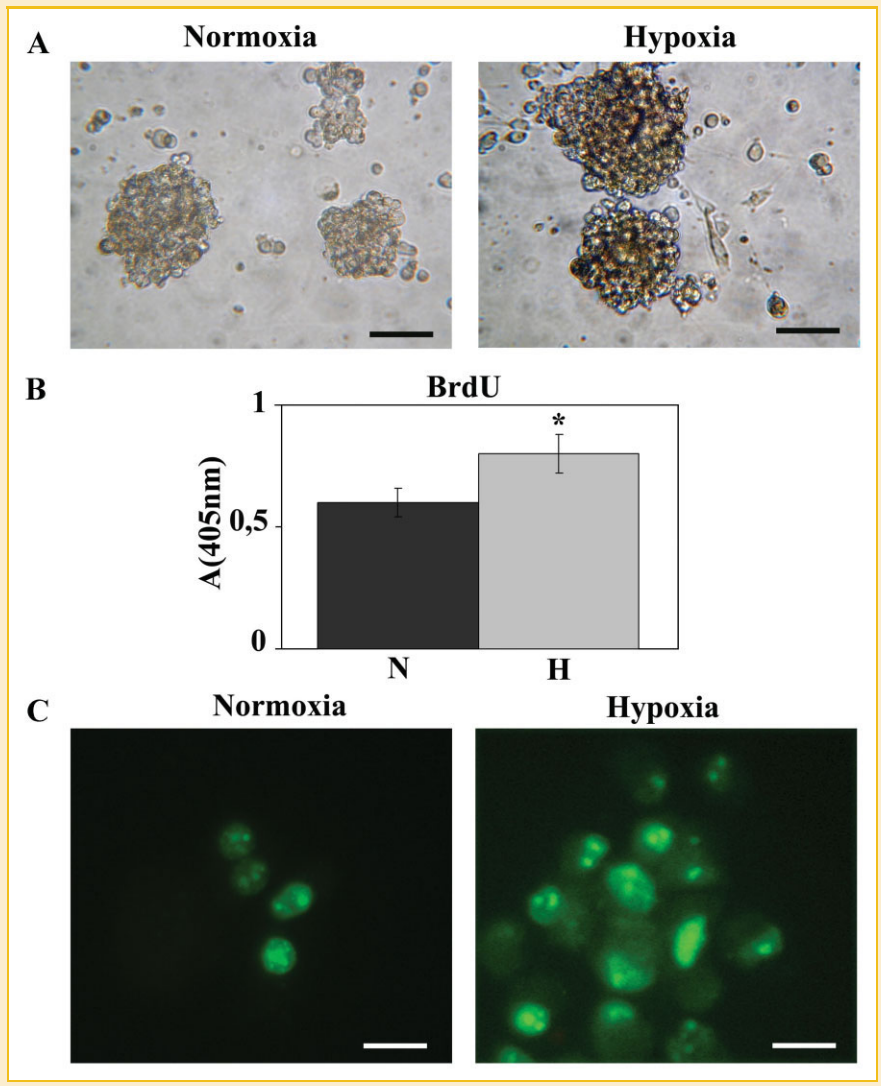

Fig. 1. Contrast phase microscopy of GB neurospheres in normoxic and hypoxic conditions (A), (Bar = 50 μm) and the proliferation assay, evaluated as BrdU incorporation (B), and immunolocalization of the proliferation marker Ki67 (C). Bar = 20 μm.

Inc., Golden, CO), mouse anti-Nestin, anti-stem cell-derived neural stem/progenitor cell supporting factor (SDNSF), anti GFAP (1:200; Chemicon International, Inc., Temecula, CA), anti-HIF-1α (1:100; Novus Biologicals, Inc. Littleton, CO). Cells were then incubated with AlexaFluor 488 conjugated goat anti-rabbit or anti mouse IgG antibodies (1:2,000; Molecular Probes, Invitrogen, Paisley, UK), for 30 min at RT. Both primary and secondary antibodies were diluted with PBS containing 3% BSA. Controls were performed by omitting the primary antibody. Cell nuclei were stained with 4′,6-diamidino-2-phenylindole (DAPI).

Coverslips, were mounted with Vectashield Mounting Medium (Vector Laboratories, Burlingame, CA) and examined at Zaiss Axioplan 2 fluorescence microscope equipped of Leica DFC 350 FX camera. Image acquistion was performed with Leica IM500 program.

BODIPY STAINING

Cells grown on coverslips after 72 h of hypoxia or normoxia were washed twice with PBS, fixed for 10 min at RT in 4% paraformaldehyde in PBS and permeabilized in PBS containing 0.1% Triton X-100 for 10 min at RT. Tumorsphere were incubated with 4,4-difluoro-1,3,5,7,8-pentamethyl 4-bora-3a,4a-diaza-s-indacene (BODIPY 493/503 Molecular Probes, Invitrogen) for 10 min at RT. A stock solution of BODIPY 493/503 1 mg/ml in ethanol was prepared and then stored at −20 in the dark until required. Before use, BODIPY stock solution was diluted 1:1,000 in PBS and used for incubate coverslips in the dark for 10 min. After incubation the cells were washed with PBS, mounted with Vectashield mounting medium and photographed at fluorescence microscope AXIOPHOT, Zeiss microscope.

LIPID EXTRACTION AND THIN LAYER CHROMATOGRAPHY

Cell pellets were dissolved in a buffer containing Tris–HCl 20 mM pH 7.4, 1 μM PMSF, 10 μM leupeptin, 10 μM pepstatin, 1 μM aprotinin. After the incubation time (5 min at 4°C), samples were sonicated (5 W, 80% output, 1 min and 50 s, altering 10 s sonication, and 10 s pause) with a Vibracell sonicator (Sonic and Materials, Inc.,

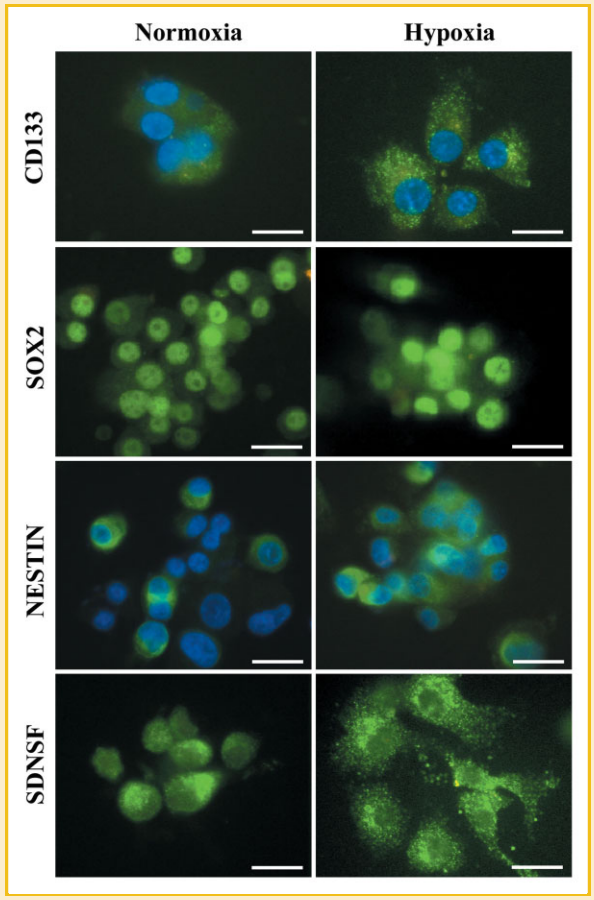

Fig. 2. Immunolocalization in normoxia and hypoxia of stemness markers such as CD133, SOX2, nestin, and the stem cell–derived neural stem/progenitor cell supporting factor (SDNSF). Bar = 20 μm.

Danbury, CT). Protein concentration of cell lysates was determined through the Bio-Rad Protein Assay (Hercules, CA), with BSA standards. Lipids were extracted by Bligh and Dyer [1959] method and applied on silica plates as thin rows at 1.5 cm distance above the bottom of the silica plate, air-dried and placed immediately in the elution tank. Eluent mixture (hexane/diethyl ether/acetic acid, 70:30:1; 100 ml) was introduced into an elution tank to separate neutral lipids. The solvent was allowed to ascend up to 3 cm from the top of the plate, and then the plate was removed, air-dried and stained. Triacylglycerol (1,2 dimyrystoil-3 palmytoil-rac-glycerol), trimyrystin, tripalmytoil (TRI), cholesterol (C), cholesteryl-ester (CE), were used as standards. TLC staining was achieved by dissolving 8% phosphomolybdic acid in ethanol and vaporized it on plates for 10 min at 80°C. TLC stained shows green/dark and green/dark blue spots on a yellow/green background. Silica plates were acquired by densitometer (UVItec Limited BTS-20M, Cambridge UK). All studies were performed in triplicate.

STATISTICAL ANALYSIS

For statistical analysis samples were processed by SPSS software and analyzed by ANOVA test. $^{*}P < 0.05$; $^{**}P < 0.005$, $^{**}P < 0.0005$. All data are mean ± SD of five separate experiments.

RESULTS

In Figure 1, contrast phase microscopy of GB neurospheres in normoxic and hypoxic conditions and the proliferation assay, evaluated as BrdU incorporation, and the immunolocalization of the proliferation marker Ki67 are shown. Hypoxia determined an increase of proliferation in GB neurospheres; in agreement, Ki67 immunolocalization shows an increase of the immunopositive cells under hypoxia.

Figure 2 shows the immunolocalization in normoxia and hypoxia of stemness markers such as CD133, SOX2, nestin, and the stem cell-derived neural stem/progenitor cell supporting factor (SDNSF). Hypoxia increases the fluorescence intensity for all the examined markers.

Figure 3 shows the cytofluorimetric analyses for CD133, SOX2, nestin, the stem cell-derived neural stem/progenitor cell supporting factor (SDNSF) and the astroglial differentiation marker GFAP in GB neurospheres, both in normoxic and hypoxic conditions. In agreement with the immunofluorescence studies all the stemness markers resulted increased, even if at different levels, by hypoxia while the differentiation marker resulted significantly decreased. Particular is the behavior of SOX2 in cytofluorimetry, in fact, the transcription factor results decrease or not significantly changed in hypoxia, as % of positive cells, but the fluorescence intensity (mean) of the positive cells resulted increased by hypoxia, thus indicating an increase of SOX2 in not all the stem cells in hypoxia. These data are confirmed by the Western blotting analysis showed in Figure 4.

In Figure 5, the immunolocalization and Western blotting analysis for the inducible hypoxia factor 1 α (HIF-1α) was investigated in GB neurospheres, both in normoxic and hypoxic conditions (A). The results obtained confirmed the establishment of the hypoxic condition by the up-regulation and nuclear localization of HIF-1α under hypoxia. At this point, in order to establish if hypoxia, as observed in primary cultures [Laurenti et al., 2011], was able to induce a lipid metabolism deregulation also in GB neurospheres, the peroxisomal proteins involved in lipid metabolism such as PMP70, Acyl-CoA oxidase (AOX), thiolase (THL), and HMGCoA-reductase (HMG-red) were assayed. In Figure 5B, the immunolocalization and Western blotting analysis for the peroxisomal membrane protein PMP70, one of the four ABC half-transporters of mammalian peroxisomes involved in fatty acid processing [Di Benedetto et al., 2008], are reported. Hypoxia strongly upregulated PMP70. In the same figure, the real-time PCR analysis for the lipid metabolism proteins, AOX, THL, HMG-red is shown. The hypoxic condition upregulated AOX, while THL and HMG-red resulted unaffected (Fig. 5C).

In agreement with the deregulation of the lipid enzymes, an increase of lipid droplets accumulation in GB neurospheres is observed under hypoxia (Fig. 6). This event was paralleled by the strong increase of cholesterol and cholesteroyl-esters observed by TLC (Fig. 6).

Since the strong involvement of PPARs in the control of lipid metabolism and due to the significant increase of PPARα found by us both in glioma specimens and glioma primary cultures, we then

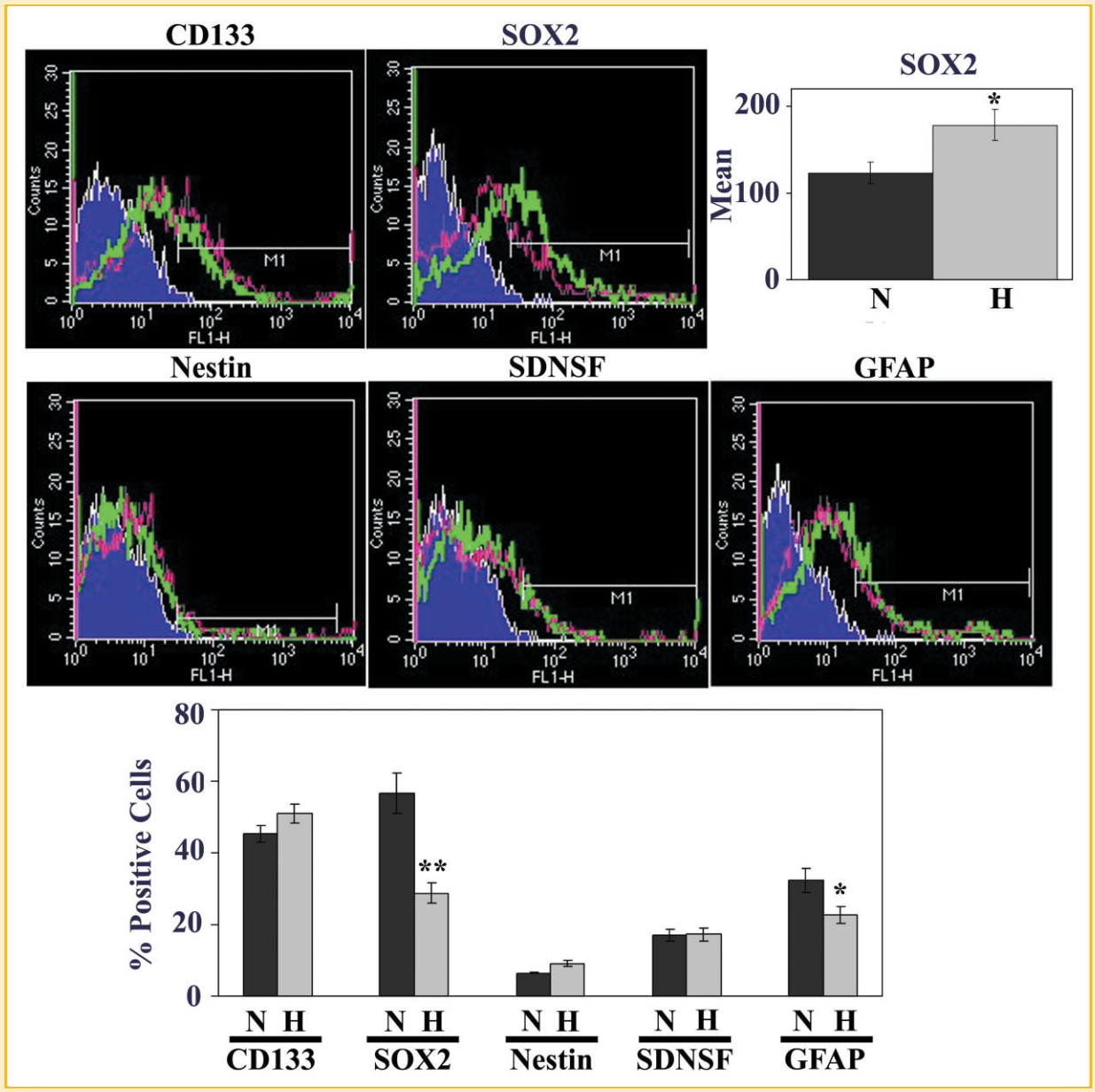

Fig. 3. Cytofluorimetric analyses for CD133, SOX2, nestin, the stem cell-derived neural stem/progenitor cell supporting factor (SDNSF) and the astroglial differentiation marker GFAP in GB neurospheres, both in normoxic and hypoxic conditions. Data are mean ± SD of five different experiments. $^{*}P < 0.05$; $^{**}P < 0.001$.

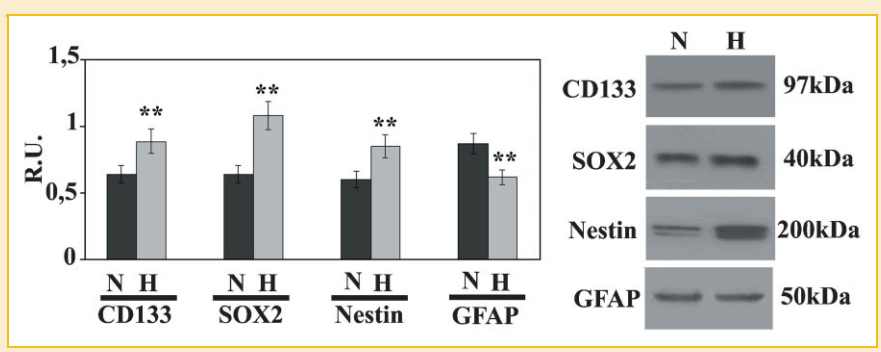

Fig. 4. Western blotting analysis for CD133, SOX2, nestin and the astroglial differentiation marker GFAP in GB neurospheres, both in normoxic and hypoxic conditions. Data are mean ± SD of five different experiments. $^{*}P < 0.05$; $^{**}P < 0.001$.

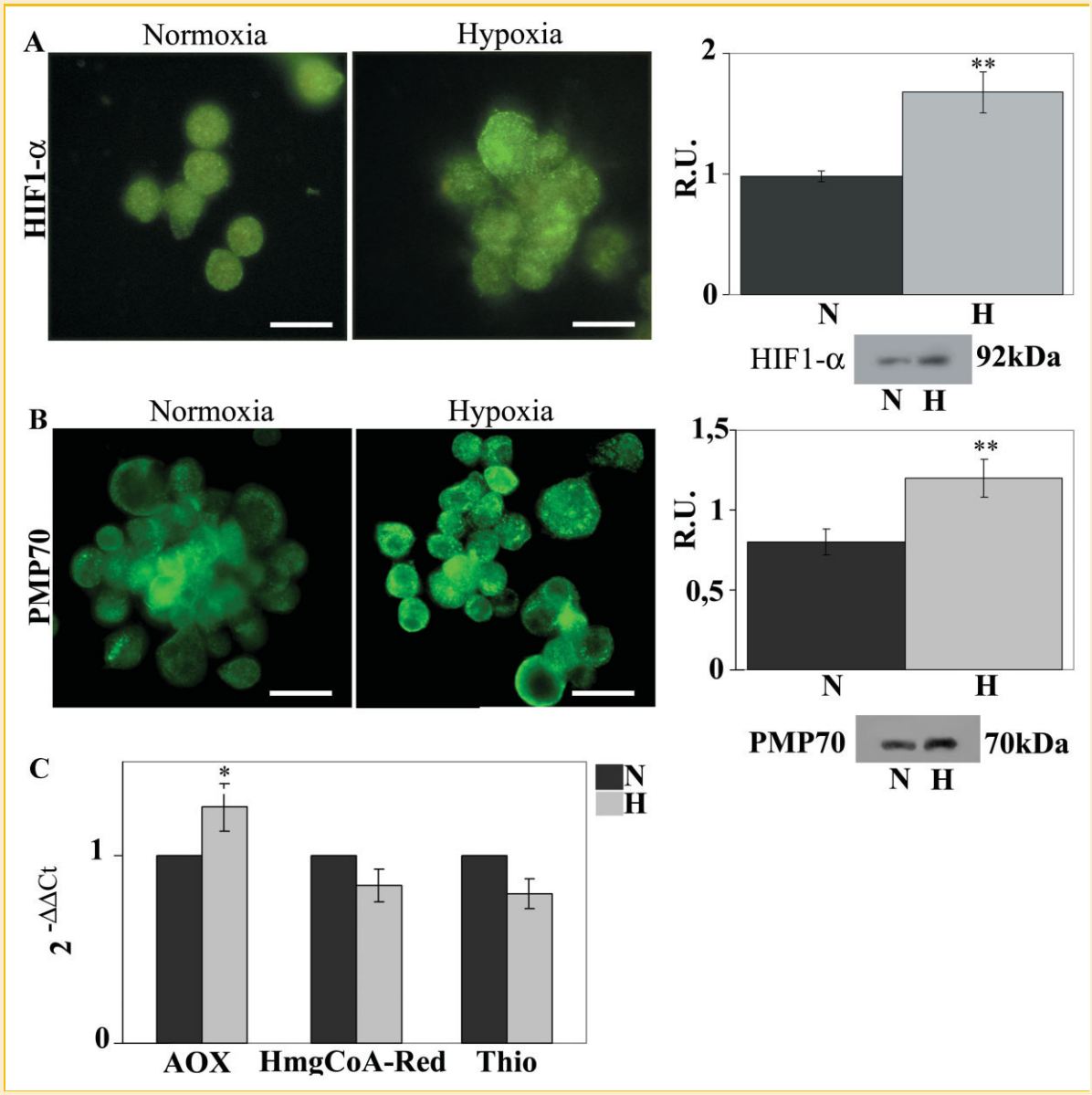

Fig. 5. Immunolocalization and Western blotting analysis for the inducible hypoxia factor 1 α (HIF-1α) was investigated in GB neurospheres, both in normoxic and hypoxic conditions (A). In panel B, the immunolocalization and Western blotting analysis for the peroxisomal membrane protein PMP70 is shown. In panel C, real-time PCR analysis for the lipid metabolism proteins, AOX, THL, HMG-red is reported. Data are mean ± SD of five different experiments. $^{*}P < 0.05$; $^{**}P < 0.001$. Bar = 20 μm.

investigated the expression of the three PPARs both in normoxia and hypoxia in GB stem cells.

In Figure 7, the immunolocalization for PPARα, β and γ is reported. Hypoxia strongly increases the fluorescence intensity for PPARα, while concomitantly decreases PPARβ and γ fluorescence intensity. In Figure 8, Western blotting and real-time PCR analyses for the three PPAR isotypes is reported. Hypoxia strongly increases PPARα at protein level, while it was uneffective on mRNA, thus suggesting a possible stabilization of the protein, in agreement with the increase of its target gene, AOX. In parallel, the expression of the other two isotypes, PPARβ and γ appeared strongly downregulated by hypoxia, both at mRNA and protein level, thus suggesting different functions for the three isotypes in GB neurospheres.

DISCUSSION

HIF-1α is master regulators of the transcriptional response to hypoxia. When a stem cell is experiencing a reduced oxygen environment, HIF-1α will induce (or inhibit) the expression of many of genes. In recent studies on GB neurospheres, HIF-1α and HIF-2α mRNAs where shown to be expressed between physiologic oxygen levels (5–7% range) to moderate hypoxia (1–2%). While HIF-2α protein is present in a wide range of oxygen levels, HIF-1α protein is restricted to cells living under moderate hypoxia. Moreover, hypoxia has been described to modulate several pathways involved in cell survival, proliferation, differentiation, and death [Bar et al., 2010].

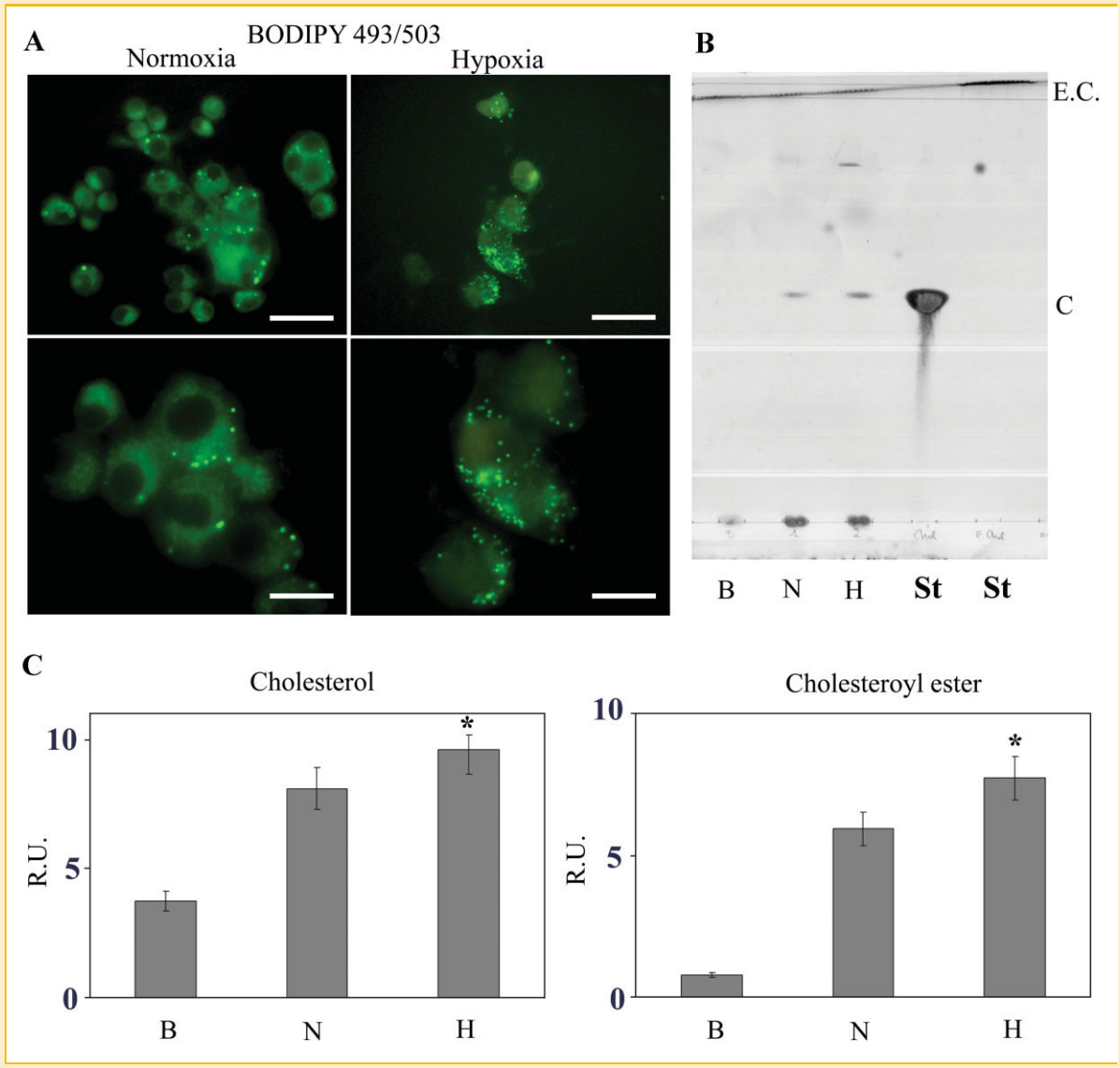

Fig. 6. Lipid droples staining in GB neurospheres in normoxia and hypoxia conditions (A). Bar = 40 μm (Top) and 20 μm (bottom). In panel B, TLC and relative densitometric analysis of lipid extracts fro GB neurospheres cultured under hypoxia and normoxia; B = bllank; N = normoxia; h = hypoxia; st = standard. Data are mean ± SD of five different experiments. $^{*}P < 0.05$.

We have recently suggested that hypoxia and HIF-1α may be responsible for lipid metabolism impairment in human gliomas. Indeed, under hypoxia, in gliomas a malignancy grade-dependent accumulation of lipid droplets, containing neutral lipids, have been previously described [Opstad et al., 2008], also confirmed by us both in ex vivo and in vitro glioblastoma specimens and cells [Benedetti et al., 2010; Laurenti et al., 2011]. As reported [Bar et al., 2010] there are several similarities between normal neural stem cells and GB stem cells in regards to their response to hypoxia. We also found a similarity as regards lipid droplets accumulation. In fact in mouse neural stem cells, under proliferative conditions, an evident accumulation of lipid droplets was observed [Cimini et al., 2007], as happens in human gliomas, with GB being the most endowed in lipid droplets, mainly under hypoxia [Laurenti et al., 2011]. In this view appears important to investigate on the expression of PPARs, the master genes involved not only in the lipid metabolism, but also in the overall energetic metabolism.

Our results show, in agreement with other authors, a hypoxia dependent up-regulation of the stemness markers with a concomitant up-regulation of lipid metabolism enzymes, cholesterol, cholestroyl-esters and of the PPARα, the transcription factor involved in their transcriptional control.

It has been previously described in many tumors alterations in lipid metabolism and the high rates of de novo fatty acid biosynthesis [Medes et al., 1953]. The cholesterol synthesis is mediated by mevalonate pathway which uses acetyl-CoA as substrate. An abnormally active de novo synthesis of cholesterol from acetate and mevalonate (MVA) in malignant glial cells, compared with their normal counterparts has been reported [Goldstein and Brown, 1990]. This pathway produces various end

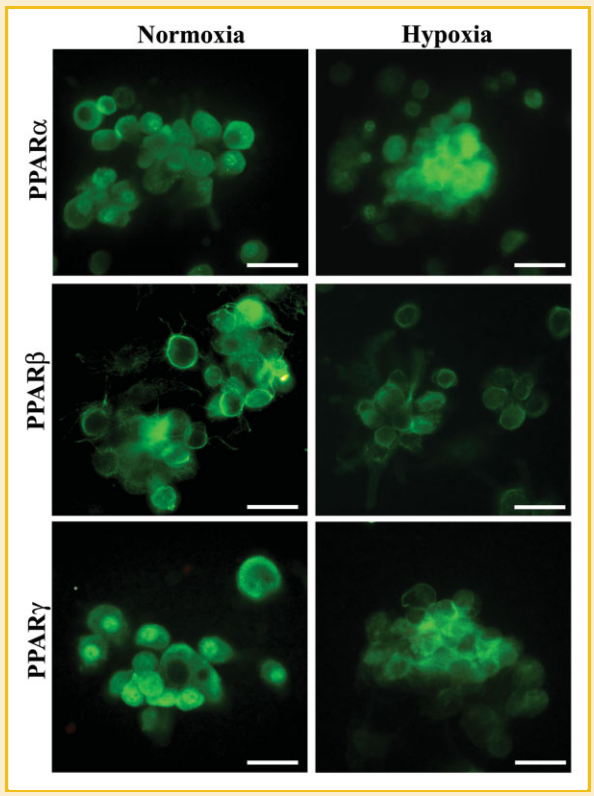

Fig. 7. PPARs immunolocalization in GB neurospheres under normoxic and hypoxic conditions. Bar = 20 μm.

products critical for both normal and cancerous cells. The rate-limiting step of this pathway is catalyzed by HMG-CoA reductase [Goldstein and Brown, 1990]. Many cancerous cells seem highly dependent on the availability of the end products of MVA pathway [Chan et al., 2003].

In this study, we evaluated the role of hypoxia on the expression profiles of several lipid metabolic enzymes and PPARs on GB neurospheres. The results obtained confirmed the upregulation of the peroxisomal proteins involved in lipid metabolism with an increase, under hypoxia, also of the lipid droplets and of the cholesterol and cholesteroyl-esters synthesis. These findings appear in agreement with the lipid metabolism perturbation previously observed in glioma specimens and in glioma primary cultures. In fact, also in GB stem cells, acyl-CoA oxidase, that catalyzed the rate-limiting step of the β-oxidation pathway with acetyl-CoA production, which constitutes the substrate for mevalonate synthesis, is significantly up-regulated by hypoxia as also supported by the increase of cholesterol and cholestroyl-esters content. These findings suggest that hypoxia and the subsequent metabolic cascade are able to affect lipid metabolism and particularly cholesterol synthesis. This is further supported by the observation, under hypoxia, of the increase and nuclear localization of PPARα, suggesting the activation of the nuclear receptor. This is further stressed by the significant increase of AOX, that is known to be under PPARα transcriptional control. This strong up-regulation of lipid metabolism, under hypoxia, may be related to the anerobic glycolitic metabolism that is known to occur in this tumor, under low oxygen levels. The glycolitic pathway produce less, but faster ATP, therefore a different pathway may be used for membrane lipid synthesis and for sustaining cell metabolism. In this view, the activation of PPARα may constitute a useful way to up-regulate cholesterol synthesis and to maintain cell proliferation. Moreover, it has been demonstrated that lipid droplets other than containing only neutral lipids, are complex structures that contain several proteins, some under PPARα transcriptional control such as adipose differentiation-related protein (ADPR) [Edvardsson et al., 2006]. These droplets may eventually constitute a simple way used by GB cells to transport informations between cells, since they are released at the foci of pseudopalisading necrosis. The Hedgehog (Hh) pathway is a major regulator of many fundamental processes in vertebrate embryonic development including stem cell maintenance, cell differentiation, tissue polarity, and cell proliferation. Constitutive activation of the Hh pathway leading to tumorigenesis is seen in basal cell carcinomas and medulloblastoma. A variety of other human cancers, including brain, gastrointestinal, lung, breast, and prostate cancers, also demonstrate inappropriate activation of this pathway. Paracrine Hh signaling from the tumor to the surrounding stroma was recently shown to promote tumorigenesis. This pathway has also been shown to regulate proliferation of cancer stem cells and to increase tumor invasiveness [Gupta et al., 2010]. It has been recently demonstrated that cholesterol metabolism is required for intracellular hedgehog signal transduction and also a requirement for intracellular cholesterol synthesis for proper regulation of Hh activity via Smoothened [Stottmann et al., 2011]. Moreover, hedgehog paracrine molecules should be palmytoylated and bound to cholesterol for its activity; many authors have raised the question how this lipophilic compound may be transported in the hydrophilic extracellular environment [Thérond, 2012]. It is possible to speculate that the abnormal cholesterol synthesis and PPARα activation that we observe, paralleled by lipid droplets increase, may constitute the way used for hedgehog activation and transport.

Several reports have discussed on the possible role of PPARs in neural stem cell proliferation, maintenance, and differentiation [Cimini et al., 2007; Cimini and Cerù, 2008], in particular PPARγ has been implicated both in proliferation and differentiation [Wada et al., 2006; Wang et al., 2011], while PPARβ has been indicated in neuroblast differentiation [D'Angelo et al., 2011]. In our experimental conditions, the strong upregulation of PPARα, with its implication on lipid metabolism, is paralleled by a significant down regulation of PPARβ and γ. This finding indicate that even if displaying similar features, neural stem cells appear different from GB stem cells. In fact, in mouse neural stem cells we found an up-regulation of PPARα only when NSC underwent to astroglial differentiation [Cimini et al., 2007] or other authors described PPARγ as crucial for NSC proliferation. Herein, it appears that is the PPARα the one involved in the maintenance and proliferation of cancer stem cells and that a downregulation of the other two PPARs is needed for maintaining these processes. For example, it is known that NFkB signaling is involved in NSC migration, in response to TNFα or hypoxia [Widera et al., 2004]; TNFα induces NFkB activation which promotes MCP1, SDF1, and SCF gene transcription,

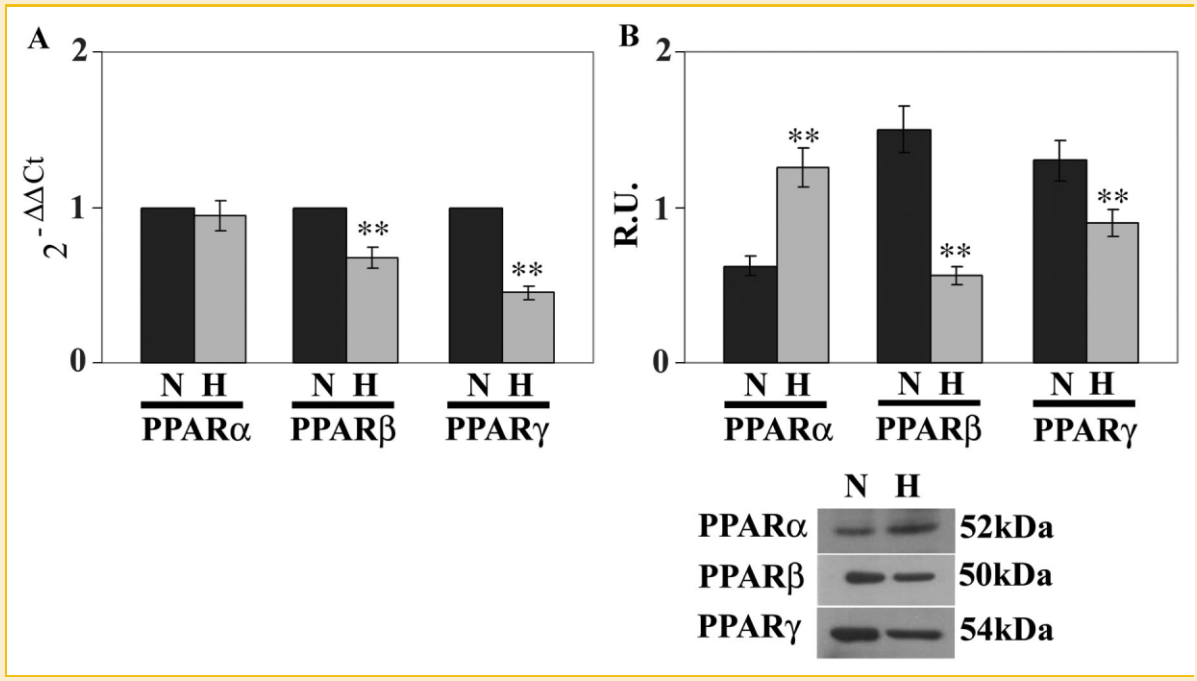

Fig. 8. Real-time PCR and Western blotting analyses of the different PPAR isotypes in GB neurospheres under normoxia and hypoxia. Data are mean ± SD of five different experiments. $^{**}P < 0.001$.

all of which are involved in migration [Da Silva et al., 2003; Sun et al., 2004; Jung et al., 2008]. PPARγ plays an inhibitory effects on this pathway inactivating TNFα signaling pathway by maintaining NFkB in inactive form [Bylund et al., 2003], thus in GB stem cells this pathway may be maintained active by the downregulation of this transcription factor.

On the overall, our data indicate that PPARα is strongly involved in GB stem cell biology, and probably malignancy, and that this implies a deregulation of the lipid metabolism and a downregulation of PPARβ and γ. Our data also suggest that hypoxia and PPARα may be directly involved in proliferation and chemoresistance, main features of cancer stem cells, suggesting the use of PPARα antagonists may represent a potential approach for counteracting chemoresistance by blocking lipid metabolism catabolism and eventually promoting cell death. On the other hand, the use of specific PPARβ or γ agonists may be suggested to increase cancer stem cell differentiation or to counteract proliferation.

REFERENCES

Amberger-Murphy V. 2009. Hypoxia helps glioma to fight therapy. Curr Cancer Drug Targets 9:381–390.

Bar EE. 2011. Glioblastoma, cancer stem cells and hypoxia. Brain Pathol 21:119–129.

Bar EE, Lin A, Mahairaki V, Matsui W, Eberhart CG. 2010. Hypoxia increases the expression of stem-cell markers and promotes clonogenicity in glioblastoma neurospheres. Am J Pathol 177:1491–1502.

Benedetti E, Galzio R, Cinque B, Biordi L, D'Amico MA, D'Angelo B, Laurenti G, Ricci A, Festuccia C, Cifone MG, Lombardi D, Cimini A. 2008. Biomolecular characterization of human glioblastoma cells in primary cultures: Differentiating and antiangiogenic effects of natural and synthetic PPARgamma agonists. J Cell Physiol 217:93–102.

Benedetti E, Galzio R, D'Angelo B, Cerù MP, Cimini A. 2010a. PPARs in human neuroepithelial tumors: PPAR ligands as anticancer therapies for the most common human neuroepithelial tumors. PPAR Res 2010:427401.

Benedetti E, Galzio R, Laurenti G, D'Angelo B, Melchiorre E, Cifone MG, Fanelli F, Muzi P, Coletti G, Alecci M, Sotgiu A, Cerù MP, Cimini A. 2010b. Lipid metabolism impairment in human gliomas: expression of peroxisomal proteins in human gliomas at different grades of malignancy. Int J Immunopathol Pharmacol 23:235–246.

Berger J, Moller DE. 2002. The mechanisms of action of PPARs. Ann Rev Med 53:409–435.

Bligh EG, Dyer WJ. 1959. A rapid method for total lipid extraction and purification. Can J Biochem Physiol 37:911–917.

Bylund M, Andersson E, Novitch BG, Muhr J. 2003. Vertebrate neurogenesis is counteracted by Sox1-3 activity. Nat Neurosci 6:1162–1168.

Chan KK, Oza AM, Siu LL. 2003. The statins as anticancer agents. Clin Cancer Res 9:10–19.

Cimini A, Cerù MP. 2008. Emerging roles of peroxisome proliferator-activated receptors (PPARs) in the regulation of neural stem cells proliferation and differentiation. Stem Cell Rev 4:293–303.

Cimini A, Ippoliti R. 2011. Innovative therapies against human glioblastoma multiforme. ISRN Oncol 2011:787490.

Cimini A, Cristiano L, Benedetti E, D'Angelo B, Cerù MP. 2007. PPARs expression in adult mouse neural stem cells: Modulation of PPARs during astroglial differentiaton of NSC. PPAR Res 2007:48242.

D'Angelo B, Benedetti E, Di Loreto S, Laurenti G, Cerù MP, Cimini A. 2011. Signal transduction pathways involved in PPARß-induced neuronal differentiation 1. J Cell Physiol 226:2170–2180.

Da Silva CA, Heilbock C, Kassel O, Frossard N. 2003. Transcription of stem cell factor (SCF) is potentiated by glucocorticoids and interleukin-1beta through concerted regulation of a GRE-like and an NF-kappaB response element. FASEB J 17:2334–2336.

Di Benedetto R, Denti MA, Salvati S, Sanchez M, Attorri L, David G, Di Biase A. 2008. RNAi-mediated silencing of ABCD3 gene expression in rat C6 glial

cells: A model system to study PMP70 function. Neurochem Int 52:1106–1113.

Di Loreto S, Corvetti L, Maccarone R, Piancatelli D, Adorno D. 2000. Interleukin 1-beta modulates the effects of hypoxia in neuronal culture. J Neuroimmunol 106:32–42.

Doherty GH. 2007. Developmental switch in the effects of TNFalpha on ventral midbrain dopaminergic neurons. Neurosci Res 57:296–305.

Dreyer C, Krey G, Keller H, Givel F, Helftenbein G, Wahli W. 1992. Control of the peroxisomal beta-oxidation pathway by a novel family of nuclear hormone receptors. Cell 68:879–887.

Edvardsson U, Ljungberg A, Linden D, William-Olsson L, Peilot-Sjogren H, Ahnmark A, Oscarsson J. 2006. PPAR-alpha activation increases triglycerides mass and adipose differentiation-related protein in hepatocytes. J Lipid Res 47:329–340.

Escher P, Wahli W. 2000. Peroxisome proliferator-activated receptors: Insight into multiple cellular functions. Mutat Res 448:121–138.

Ezashi T, Das P, Roberts RM. 2005. Low O_2 tensions and the prevention of differentiation of hES cells. Proc Natl Acad Sci USA 102:4783–4788.

Feige JN, Gelman L, Michalik L, Desvergne B, Wahli W. 2006. From molecular action to physiological outputs: Peroxisome proliferator-activated receptors are nuclear receptors at the crossroads of key cellular functions. Progr Lipid Res 45:120–159.

Garza JC, Guo M, Zhang W, Lu XY. 2008. Leptin increases adult hippocampal neurogenesis in vivo and in vitro. J Biol Chem 283:18238–18247.

Gearing KL, Gottlicher M, Teboul M, Widmark E, Gustafsson JA. 1993. Interaction of the peroxisome-proliferatoractivated receptor and retinoid X receptor. Proc Natl Acad Sci USA 90:1440–1444.

Goldstein JL, Brown MS. 1990. Regulation of the mevalonate pathway. Nature 343:425–430.

Guillemot F. 2007. Cell fate specification in the mammalian telencephalon. Prog Neurobiol 83:37–52.

Gupta S, Takebe N, Lorusso P. 2010. Targeting the Hedgehog pathway in cancer. Ther Adv Med Oncol 2:237–250.

Issemann I, Green S. 1990. Activation of a member of the steroid hormone receptor superfamily by peroxisome proliferators. Nature 347:645–650.

Jensen RL. 2009. Brain tumor hypoxia: Tumorigenesis, angiogenesis, imaging, pseudoprogression, and as a therapeutic target. J Neurooncol 92:317–335.

Jung Y, Song S, Choi C. 2008. Peroxisome proliferator activated receptor γ agonists suppress TNFα-induced ICAM-1 expression by endothelial cells in a manner potentially dependent on inhibition of reactive oxygen species. Immunol Lett 117:63–69.

Keller H, Dreyer C, Medin J, Mahfoudi A, Ozato K, Wahli W. 1993. Fatty acids and retinoids control lipid metabolismthrough activation of peroxisome proliferator-activated receptor–retinoid X receptor heterodimers. Proc Natl Acad Sci USA 90:2160–2164.

Krey G, Braissant O, L'Horset F, Kalkhoven E, Perroud M, Parker MG. 1997. Fatty acids, eicosanoids, and hypolipidemic agents identified as ligands of peroxisome proliferator activated receptors by coactivator-dependent receptor ligand assay. Mol Endocrinol 11:779–791.

Laurenti G, Benedetti E, D'Angelo B, Cristiano L, Cinque B, Raysi S, Alecci M, Cerù MP, Cifone MG, Galzio R, Giordano A. 2011. Cimini A Hypoxia induces peroxisome proliferator-activated receptor α (PPARα) and lipid metabolism peroxisomal enzymes in human glioblastoma cells. J Cell Biochem 112: 3891–3901.

Livak KJ, Schmittgen TD. 2001. Analysis of relative gene expression data using real-time quantitative PCR and the 2(-Delta Delta C(T)) method. Methods 25:402–408.

McCord AM, Jamal M, Shankavaram UT, Lang FF, Camphausen K, Tofilon PJ. 2009. Physiologic oxygen concentration enhances the stem-like properties of CD133+ human glioblastoma cells in vitro. Mol Cancer Res 7:489–497.

Medes G, Thomas A, Weinhouse S. 1953. Metabolism of neoplastic tissue. IV. A study of lipid synthesis in neoplastic tissue slices in vitro. Cancer Res 13:27–29.

Morales-Garcia JA, Luna-Medina R, Alfaro-Cervello C, Cortes-Canteli M, Santos A, Garcia-Verdugo JM, Perez-Castillo A. 2011. Peroxisome proliferator-activated receptor γ ligands regulate neural stem cell proliferation and differentiation in vitro and in vivo. Glia 59:293–307.

Nuclear Receptor Nomenclature Committee. 1999. A unified nomenclature system for the nuclear receptor superfamily. Cell 97:161–163.

Opstad KS, Bell BA, Griffiths JR, Howe FA. 2008. An investigation of human brain tumour lipids by high-resolution magic angle spinning 1H MRS and histological analysis. NMR Biomed 21:677–685.

Panchision DM. 2009. The role of oxygen in regulating neural stem cells in development and disease. J Cell Physiol 220:562–568.

Pistollato F, Chen HL, Rood BR, Zhang HZ, D'Avella D, Denaro L, Gardiman M, te Kronnie G, Schwartz PH, Favaro E, Indraccolo S, Basso G, Panchision DM. 2009. Hypoxia and HIF1alpha repress the differentiative effects of BMPs in high-grade glioma. Stem Cells 27:7–17.

Sahlgren C, Gustafsson MV, Jin S, Poellinger L, Lendahl U. 2008. Notch signaling mediates hypoxia-induced tumor cell migration and invasion. Proc Natl Acad Sci USA 105:6392–6397.

Sathornsumetee S, Cao Y, Marcello JE, Herndon JE II, McLendon RE, Desjardins A, Friedman HS, Dewhirst MW, Vredenburgh JJ, Rich JN. 2008. Tumor angiogenic and hypoxic profiles predict radiographic response and survival in malignant astrocytoma patients treated with bevacizumab and irinotecan. J Clin Oncol 26:271–278.

Smith PK, Krohn RI, Hermanson GT, et al. 1985. Measurement of protein using bicinchoninic acid. Anal Biochem 150:76–85.

Soeda A, Park M, Lee D, Mintz A, Androutsellis-Theotokis A, McKay RD, Engh J, Iwama T, Kunisada T, Kassam AB, Pollack IF, Park DM. 2009. Hypoxia promotes expansion of the CD133-positive glioma stem cells through activation of HIF-1alpha. Oncogene 28:3949–3959.

Stottmann RW, Turbe-Doan A, Tran P, Kratz LE, Moran JL, Kelley RI, Beier DR. 2011. Cholesterol metabolism is required for intracellular hedgehog signal transduction in vivo. PLoS Genet 7:e1002224.

Sun L, Lee J, Fine HA. 2004. Neuronally expressed stem cell factor induces neural stem cell migration to areas of brain injury. J. Clin. Invest 113:1364–1374.

Thérond PP. 2012. Release and transportation of Hedgehog molecules. Curr Opin Cell Biol 24:173–180.

Vaupel P, Mayer A. 2007. Hypoxia in cancer: Significance and impact on clinical outcome. Cancer Metastasis Rev 26:225–239.

Wang SH, Guo YJ, Yuan Y, Li L, Li FF, Ye KP, Huang Y. 2011. PPARγ-mediated advanced glycation end products regulate neural stem cell proliferation but not neural differentiation through the BDNF-CREB pathway. Toxicol Lett 206:339–346.

Wada K, Nakajima A, Katayama K, Kudo C, Shibuya A, Kubota N, Terauchi Y, Tachibana M, Miyoshi H, Kamisaki Y, Mayumi T, Kadowaki T, Blumberg RS. 2006. Peroxisome proliferator-activated receptor γ-mediated regulation of neural stem cell proliferation and differentiation. J Biol Chem 81:12673–12681.

Widera D, Holtkamp W, Entschladen F, Niggemann B, Zänker K, Kaltschmidt B, Kaltschmidt C. 2004. MCP-1 induces migration of adult neural stem cells. Eur J Cell Biol 83:381–387.

Wolfrum C, Borrmann CM, Borchers T, Spener F. 2001. Fatty acids and hypolipidemic drugs regulate peroxisome proliferator-activated receptors alpha- and gamma-mediated gene expression via liver fatty acid binding protein: A signaling path to the nucleus. Proc Natl Acad Sci USA 98:2323–2328.

Yu SC, Ping YF, Yi L, Zhou ZH, Chen JH, Yao XH, Gao L, Wang JM, Bian XW. 2008. Isolation and characterization of cancer stem cells from a human glioblastoma cell line U87. Cancer Lett 265:124–134.